AD-A165 671 A NUMERICAL STUDY OF THE AERODYNAMIC INTERFERENCE OF A 1/1
MODEL SUPPORT SYST (U) ROYAL AIRCRAFT ESTABLISHMENT
FARNBOROUGH (ENGLAND) B C HARDY SEP 85
UNCLASSIFIED RAE-TM-AERO-2046 DRIC-BR-97527 F/G 14/2 NL

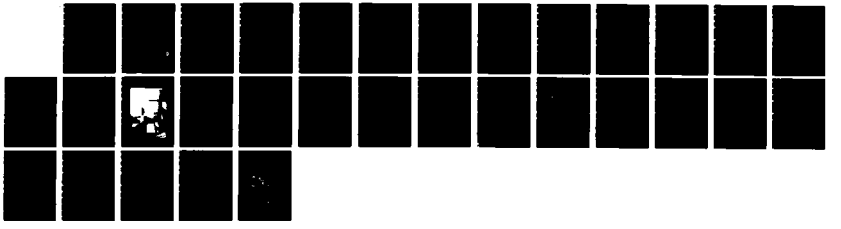

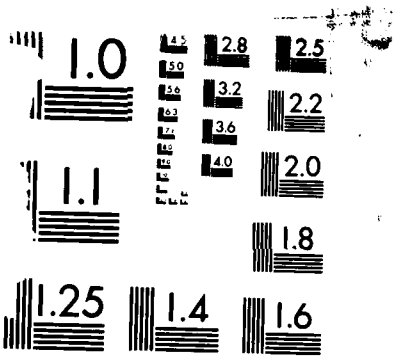

TECH. MEMO
AERO 2046

UNLIMITED

10-12-85
DMB.

TECH. MEMO
AERO 2046

REPRINT

ROYAL AIRCRAFT ESTABLISHMENT

A NUMERICAL STUDY OF THE AERODYNAMIC INTERFERENCE OF A MODEL SUPPORT SYSTEM USED IN THE RAE 5 METRE WIND TUNNEL

by

B. C. Hardy

September 1985

Procurement Executive, Ministry of Defence
Farnborough, Hants

UNLIMITED

ROYAL AIRCRAFT ESTABLISHMENT

Technical Memorandum Aero 2046

Received for printing 5 September 1985

A NUMERICAL STUDY OF THE AERODYNAMIC INTERFERENCE OF A MODEL SUPPORT SYSTEM USED IN THE RAE 5 METRE WIND TUNNEL

by

B. C. Hardy

SUMMARY

Some aspects of the lift interference effects of support systems for wind-tunnel models have been investigated using panel method calculations. The mechanisms involved have been clarified and comparison with experimental results for a large civil transport model in the RAE 5 metre Tunnel is encouraging.

Keywords: Great Britain, charts, Subsonic flow, aerodynamic characteristics.

LIST OF CONTENTS

1 INTRODUCTION

The advent of large, low-speed pressurised wind tunnels, such as the 5 metre Wind Tunnel at RAE Farnborough, has made possible the testing of models at, or very near, full-scale conditions. The results from such tests are relevant in making direct flight/tunnel comparisons and in predicting the full-scale aerodynamics of new designs.

However, before the results of such wind-tunnel tests can be used in this manner, corrections must be applied to them to account for the constraining effects of tunnel walls, tare loads on the model support system and its aerodynamic interference at the model, etc. With the capability of testing at near full-scale conditions, the accurate determination of these corrections is of paramount importance.

Kirby *et al*[1] report a series of experiments aimed at isolating various aspects of support-rig interference for the A300B and Hawk aircraft models in the 5m Wind Tunnel. This work was time-consuming and difficult, and any contribution to the determination of these effects through the use of computational methods would clearly be very useful.

The main strut guards were identified as a major source of lift interference for the A300B model in Ref 1 and the present work is aimed at clarifying this particular aspect of the problem through calculation of the mutual interference between the wing and the main strut guards. As described in Ref 1 an attempt was made to calculate this effect using simple line-vortex models and the Maskew[2] vortex lattice program. The present calculations use a much more versatile panel program, SPARV, which is described in Ref 3.

A brief summary of the relevant results from Ref 1 is given in section 2 and the approach adopted and assumptions made in the present work are detailed in section 3. The results of some preliminary calculations made using a simplified geometry to clarify the various sources of interference are discussed in section 4. The predicted lift interference for the A300B model is compared to the measured values from Ref 1 in section 5, the results are discussed in section 6 and finally some conclusions are drawn in section 7.

2 RESULTS FROM REF 1

Ref 1 describes the results of tests made using the 1/13 scale A300B model. They were obtained by mounting the model on a strain-gauge balance on a sting, then testing the model with the guards appropriate to strut support rigs fixed to the tunnel floor under the wing of the model, then testing again with the guards removed. The interference effect of the guards was obtained by differencing the results of the two tests. Force and pressure data were taken. Fig 1 shows one of the many configurations tested. Ref 1 presents results for a number of trailing-edge flap configurations and for incidences up to and beyond the stall. It was found that the main strut guards contributed the major portion of the lift interference effect, amounting to about 1.5% of the total lift at a wing lift coefficient of 2.3. Two mechanisms for this interference were identified; the flow displacement effect of the strut guards and the mutual lift interference between the guards and the wing.

The displacement effect of the strut guards results from the flow about the guards inducing upwash and streamwash (flow acceleration) at the wing. This effect is well-known, and a method of correcting for it has been proposed. This involves measuring (or calculating) the flow about the guards in the absence of the model, and evaluating a mean

upwash and streamwash in the plane of the wing. Thus one set of flowfield data can be applied to a range of tests. An example of this technique is given in Ref 4.

The mutual lift interference between the wing and strut guards is a little more subtle, as Ref 1 points out. When the model is producing lift, the wing induces a sidewash at the guards position, thus placing the guard at an angle of attack. The guards themselves then produce lift (or, more precisely, sideforce), and thus have a trailing vortex wake. This trailing (and bound) vorticity induces velocities back at the wing, and alters the flow there. However, after subtracting the usual wind-tunnel blockage correction the results from Ref 1 could be accounted for by an effective incidence correction ($\overline{\Delta\alpha}$) induced at the model by the lift interference effect alone. That is, by the trailing vortex system from the strut guard arising through the sideforce induced on the guards by the trailing vortex system of the wing (see Fig 2). The values of $\overline{\Delta\alpha}$ were deduced from the measured C_L and $dC_L/d\alpha$ values and were found to be approximately proportional to C_L as shown by Fig 3 (Fig 15 from Ref 1). Also shown in this Figure is an example of the measured ΔC_L variation with α which shows that the interference reaches a maximum and subsequently falls with increasing α. This was attributed to the reduction in lift-curve slope, $dC_L/d\alpha$, which starts well before the stall. It was noted that any upwash due to the displacement effect of the strut guard must be small or cancelled by other effects because the $\overline{\Delta\alpha}$ at $C_L = 0$ was very small. However, Ref 1 also noted that the proposed mutual lift interference mechanism was not consistent with the line vortex and vortex lattice calculations that had been carried out. Specifically, the predicted sideforce induced at the guard by the main wing lift was insufficient to produce the observed level of interference at the wing, but it was consistent with the observed deflection of the guard. Ref 1 concluded that further work, both theoretical and experimental, was required to unravel the important mechanisms.

3 CALCULATION METHOD

The results reported here were obtained using the SPARV panel method, which is described in Ref 3. The method uses distributions of sources and doublets placed on quadrilateral panels approximating the air-swept surfaces of the configuration being modelled. A 'thin-wing' option is available, which uses doublets alone placed on the camber surface and thus models only the lifting effects. The input requirements of the method are simple but offer considerable flexibility so that the present combination of lifting wings and strut guards presented little difficulty. However, the wind-tunnel walls were not represented in the present study, and so some consideration must be given to the constraining effects of the tunnel walls on results from a 'free-air' calculation.

The effect of the tunnel floor can be simulated by reflecting the model and strut guard in the tunnel floor. Calculations were therefore carried out for the wing and its reflection in the floor, with and without the strut guards (and their reflections) present. The interference effect of the guards was obtained by differencing the results. It should be emphasised that this procedure extracts only the interference effects - an 'in tunnel' calculation would also include some element of tunnel blockage, depending on the modelling of the wakes. For the present exercise, the blockage is considered

separately and computed, by the method described in Ref 5, as a correction to the mean tunnel speed when comparing theory and experiment. A further effect of the tunnel walls which is not included in the present study is the sidewash (and hence sideforce) induced on the strut guards by the lift constraint effect of the tunnel walls. This would reduce the strut sideforce slightly.

As the calculations involve interference between relatively remote components (whose closest spacing is of the order of a chord length) some simplification was justified in the model representation. The fuselage was not represented, and the wing was represented by the gross planform. The thickness distribution of the wing was represented by an RAE 100 aerofoil section, scaled to an appropriate thickness/chord ratio, and the flap system of the A300 wing was approximated by a full span trailing-edge droop with a representative chord extension. This allowed representative values for the lift-curve slope, $dC_L/d\alpha$, to be obtained, along with a realistic zero-lift incidence in the calculations.

In initial calculations, the reflection of the strut guards and wing in the tunnel floor were omitted, to reduce the number of panels required in a preliminary exploration of the problem.

Because of the relatively large spacing between components in the problem, a fairly coarse panelling scheme was used, with typically 11 panels across the chord. The linear vorticity option (the more accurate of the available options in SPARV) was used throughout. Vortex wakes shed by lifting components were not relaxed, the wakes being allowed to extend downstream parallel to the undisturbed freestream, without rolling up.

4 INITIAL CALCULATIONS

A few preliminary calculations were conducted using a much simplified representation of the A300 geometry (thin wing, no reflection in a ground plane), to establish whether the results of Ref 1 could be reproduced, at least qualitatively when only the side force effect of the strut guards was represented, *ie* only a 'thin' strut was used, with no displacement effects due to thickness. The results were quite different in character to what was expected from examining the experimental results, as the interference lift, ΔC_L , was calculated to be negative for all but the lowest wing lift, and the variation of ΔC_L with wing lift was not monotonic. Some examples of these results are given in Fig 4, which shows the spanwise variation of ΔC_l across the wing for different values of wing lift coefficient. Further calculations were carried out, but this time thickness was represented on the strut guards, and these results gave a positive interference lift, but the variation was still not monotonic - ΔC_L reached a maximum at moderate wing C_L , and then decreased with increasing wing lift. The effects of increasing the number of panels, varying the combination of trailing-edge droop and incidence of the wing, closing the tip of the strut guard and including reflections in a ground plane were all investigated, but found to have little qualitative effect on the results. Therefore, before proceeding to a more accurate representation of the A300 geometry, it was necessary to obtain a satisfactory physical explanation of the results obtained thus far.

The mechanism for mutual lift interference between strut guard and wing, as proposed in Ref 1, is the result of velocities induced by the trailing-vortex wake of the

main guards. As shown schematically in Fig 2, these velocities are seen at the wing as predominantly an upwash over the inboard part of the wing, and a downwash outboard. These velocities are proportional to the circulation about the guard, and hence to the guard side force. The guard side force is, in turn, proportional to the effective incidence of the guard, induced by the sidewash of the wing. Therefore, the interference lift on the wing, induced by the upwash from the guard, is proportional to the wing lift, and thus ΔC_L is proportional to C_L in this case. We thus write

$$\Delta C_L = K C_{YG} ,$$

where C_{YG} is the guard sideforce, and K is proportional to the lift-curve slope of the wing.

There is also the possibility that the bound vorticity on the strut guard may induce a streamwash (local flow acceleration or deceleration) over the wing. This would produce an interference lift that was proportional to the product of the guard lift and wing lift, *ie* a quadratic variation. To examine this possibility further, calculations were performed using an isolated thin strut guard, set at incidence to give the right level of sideforce, and the velocities induced in the plane of the wing were evaluated. These calculations revealed that the streamwash was likely to be too small to account for the nonlinear behaviour of the interference lift, and would give a spanwise distribution of interference lift that was different to that found in the earlier calculations - the streamwash interference being largest at the centreline of the wing, while the lift interference was observed to be largest (negative) near the strut guard position (see Fig 4). However, the calculations for the isolated, lifting thin guard revealed that there was an appreciable sidewash interference velocity arising from the trailing vortex system of the strut guard. This suggested a possible mechanism for the nonlinear interference effect.

Considering the wing bound vorticity, made up of vortex elements of typical strength, strength γ , say, the force components on the wing are given by terms of the form $\rho q \gamma$, where the velocity, q , is taken normal to the vortex element. On a swept wing a sidewash interference velocity gives rise to a velocity component normal to the bound vortex lines, and hence produces an interference lift force which is of the required sign, *ie* negative for an aft swept wing. Such a contribution to the interference lift would have a maximum near the strut guard, as required.

To test this hypothesis, an idealised configuration was modelled with a simple, untapered swept wing of zero thickness, and a thin strut guard placed below it but well upstream (see Fig 5). The wing lift could thus be altered without affecting the guard side force, which was obtained by inclining the guard to the freestream. The guard side force, and hence vorticity, was then decoupled from the wing lift. The interference at the wing is due to the trailing vorticity from the guard, and comprises the expected upwash/downwash contribution and the sidewash contribution. The upwash produces an interference lift that is simply proportional to the guard side force, that is $\Delta C_L \propto C_{YG}$, while the contribution from the sidewash gives an interference lift that is proportional to the product of the wing lift and guard side force, *ie* $\Delta C_L \propto C_L C_{YG}$.

Thus, by keeping the guard side force fixed (by keeping it at fixed incidence), and varying the wing lift by changing the trailing-edge droop, the sidewash contribution to the interference lift could be isolated as a linear reduction in ΔC_L with increasing wing lift, C_L. (Variations in the interference effect due to the changing geometry of the wing should be small.) As a more complete test of the hypothesis that the sidewash velocities lead to important interference effects, three sweep angles were tried: -30 deg, 0 deg and 30 deg. According to the hypothesis, the interference lift should be negative for the aft swept wing, zero for the unswept wing, and positive for the forward swept wing. The actual results of the calculations are shown in Fig 6. The interference lift at 'zero' wing lift is due to the upwash from the trailing vorticity of the strut guard. The variation of interference lift with wing lift is due solely to the sidewash effect, and is seen to have a variation consistent with the hypothesis. The slow reduction in interference lift for the unswept case is due to the streamwise components of vorticity that are present in the wing, particularly near the tip. This is confirmed by Fig 6c, which shows the spanwise variation of interference lift.

With the importance of the nonlinear mutual lift interference now confirmed, the overall interference effect on lift can be identified as follows:

Due to strut guard side force -

(a) $\Delta C_L \propto C_{YG}$ (upwash effect);

(b) $\Delta C_L \propto C_{YG}\, C_L$ (sidewash and streamwash effect).

Due to strut guard displacement effect (thickness) -

(a) ΔC_L = constant (upwash)

(b) $\Delta C_L \propto C_L$ (streamwash).

Also, $C_{YG} \propto C_L$, so that the total lift interference is of the form:

$$\Delta C_L = K_1 + K_2 C_L + K_3 C_L^2 \quad ,$$

where K_1 and the upwash dependent contribution to K_2 are proportional to the wing lift-curve slope, while the magnitude and sign of K_3 depends upon the wing sweep.

With the interference mechanisms now clarified, the aim of calculating the strut guard lift interference for an A300 model in the 5 metre Tunnel was pursued, and the results from these calculations are described in the next section.

5 EXPERIMENT/CALCULATION COMPARISON FOR A300B

The geometry and panelling arrangement used in the calculations is illustrated in Fig 7, which shows the wing set at 20 deg incidence and with the trailing-edge drooped at 20 deg. As previously described the wing thickness distribution was represented by an RAE100 section scaled to an appropriate thickness/chord ratio. Trailing-edge droop angles of 0, 10, 20 and 30 deg and wing incidences up to 30 deg were employed to generate the required lift. A 20% chord extension was incorporated in the cases with non-zero droops. Using these values, lift and lift-curve slopes were obtained which were representative of those obtained in the experiments described in Ref 1, in particular the 10 deg droop calculation agreed well in this respect with the 'flaps 15/8'

measurements. The strut guard geometry was accurately represented (35% RAE100), but the tip was left open after initial calculations had showed that closing it had little effect on the results. Where comparisons are made between calculation and experiment in the remainder of this section the experimental results are corrected for the wing-tunnel blockage of the main guards by application of the factor 1.0051 to the lift coefficient, as used in Ref 1.

To illustrate the relative importance of the mutual lift interference and the displacement effect for the present configuration some calculations were carried out using the 'thin wing' representation of the strut guards to give the lift effect alone. The displacement effect was taken to be the difference between the total (thick, lifting guards) and lift only (thin, lifting guards) calculations at the same guard sideforce. To further illustrate some of the displacement effects velocities at the wing induced by the thick (non-lifting) guards in the absence of the wing were calculated and these are shown in Fig 8. Results are shown for three spanwise positions - centre-line, guard and tip - and for a range of streamwise locations. Both the upwash and streamwash are largest for the guard position as might be expected. The streamwash effect is positive over the whole of the wing though there are large variations across the chord towards the root. By casual inspection of Fig 8a lift contribution of around 0.5% might be expected from this effect. The upwash position is more complex, the root chord experiences a wholly positive upwash, though with a large chordwise variation, at the guard position the upwash gradient is again large and the rear of the chord experiences downwash and at the tip the interference is wholly downwash. It is not easy to estimate the net contribution to the interference lift merely by looking at Fig 8 because of these wide variations and the effect of the chord weighting on the overall ΔC_L . Fig 9 shows the net effect, however, to be small ($\Delta C_L = 0.003$) whereas the net effect from the streamwash is shown to be actually 0.75%. Also shown in Fig 9 is the total lift interference (for the 10 deg droop case) and the contribution of the negative quadratic effect is apparent, giving rise to a maximum in the $\Delta C_L - C_L$ relationship. Bearing in mind the geometry (incidence) and lift-curve slope variations with C_L this relationship can be quite well represented by a quadratic with constant coefficients, as an example in Fig 9 shows. It is apparent from this Figure that the use of the displacement effect only would result in a rather poor prediction of the overall lift interference up to a C_L of about 2.0 and to a progressively poorer prediction at C_L greater than 2.5 but with good prediction close to $C_L = 2.25$, where the curves cross. However, Fig 10 shows that even when the displacement effect accounts for nearly all the net lift interference ($C_L = 2.5$) the spanwise variation (ΔC_ℓ) is very poorly predicted. Thus it is clear that both the mutual lift interference and the displacement effect are important for the present configuration.

The total calculated lift interference is compared to measured values from Ref 1 in Fig 11. There is some effect on the calculated values of the trailing-edge droop angle and this is indicated in the Figure. Results for two different flap configurations from Ref 1 are shown along with the result deduced from the mean line (all flap angles) of Fig 3 by application of the measured lift-curve slope values for the 'flaps 15/8' configuration. The results of Ref 1 show some peculiar effects at low C_L , apparently due

to large effective lift-curve slopes arising from flow separation phenomena on the high-lift system. This is excluded from the comparison of Fig 11, the effect would be to increase the experimental mean line ΔC_L values somewhat at low C_L. The calculation reproduces the trend of the experiment quite well and the maximum levels are reasonably predicted. There is a discrepancy at lower C_L values where the calculation seems to over-predict the interference. However, there is considerable uncertainty in the experimental data in this region as evidenced by the differences between the different flap configurations and the mean line. The slope of the mean line (that is K_2 in equation (1)) is very close to that of the calculation at $C_L = 0$ (0.0148) and it is interesting to note that the lift effect alone gives about 0.0072 and the displacement effect alone about 0.0076 for this slope (Fig 9). The main discrepancy between experiment and calculation is the much more rapid fall off of the experimental data at high C_L. This behaviour is explained in Ref 1 as being a consequence of the reduction in lift-curve slope at high C_L, a point which is discussed further in section 6.

A comparison between the measured and predicted spanwise distribution of lift interference is shown in Fig 12 for a particular case. The experimental values are from the investigation of Ref 1 though not published in that work. They were obtained by chordwise integration of pressure measurements. The trends are reasonably well predicted by the calculation but the levels over the outer wing are substantially under-predicted and the peak is quite poorly represented. The experimental values are strongly affected inboard by the reduction in wing loading due to the engine cut-out in the flap. The effect of crudely correcting the calculation for this by scaling by the ratio of the experimental to theoretical section lift coefficients is shown. Some improvement is apparent inboard but the poor prediction outboard is unaffected. It is worth noting that the rather large differences between measurement and calculation shown by Fig 12 still give quite good agreement in overall ΔC_L because of the close agreement inboard and the effect of chord weighting on the overall value.

As a final comparison between experiment and calculation the overall lift interference measured and calculated with the strut guards toed-in by 5 deg is shown in Fig 13. These measurements were made by Kirby in an attempt to clarify the interference mechanism. Once again the agreement is quite reasonable though here the stall clearly intervenes before the quadratic term in the calculation starts to reduce the interference.

6 DISCUSSION

The calculations have established the important mechanisms for the lift interference arising from the strut guards and shown the situation to be more complex than suggested in Refs 1 and 4. It is clear from the results that neither the mutual lift nor the displacement effects by themselves adequately predict the interference - the calculation/experiment comparison for A300B is in much better agreement when both are represented. Nevertheless, the calculations do not reproduce the experimental behaviour as well as hoped. As Fig 11 shows the fall off at high C_L is not well represented and neither is the behaviour at low C_L. The experimental results tend to behave in a peculiar fashion at lower C_L when compared with the data shown in Fig 11, as indicated by the example in Fig 3. However, this effect is nearly eliminated by the assumption of a linear

approximation to the mean $\overline{\Delta\alpha} - C_L$ measurements (Fig 3) and would make only a slight difference to the mean $\Delta C_L - C_L$ relationship shown in Fig 11. Thus at low C_L we are left with rather large discrepancies between the mean line from Ref 1 and the individual results for different flap configurations, though the mean line agrees quite well with the calculations, particularly as regards the slope at $C_L = 0$.

Returning to the differences at high C_L , Kirby *et al* suggest that the rapid fall in C_L is caused by the decrease in $dC_L/d\alpha$ as the stall is approached. The calculations also show a fall in ΔC_L but this is due to the quadratic term in equation (1) and is much more gentle. However, as mentioned in section 4, the coefficients K_1 and K_2 in equation (1) depend on $dC_L/d\alpha$ and so the effects of incorporating the experimental values of this parameter into the quadratic fit shown in Fig 9 was investigated. The $dC_L/d\alpha$ dependencies of K_1 and K_2 were deduced from the separate lift and displacement effect calculations (Fig 9) and are shown in the modified quadratic representation of the interference lift in Fig 14. The full experimental result (for 'flaps 15/8') is compared to the modified equation (for 10 deg droop) in this Figure and it is clear that the use of the experimental values results in a better representation of the rapid reduction in ΔC_L at high C_L . However, as noted above, the effect at low C_L is small and actually results in poorer agreement with experiment. It is worth noting here that this agreement on the powerful influence of $dC_L/d\alpha$ at higher C_L is further confirmation that the displacement effect alone cannot adequately represent the interference because of the comparatively small value of the $dC_L/d\alpha$ dependent term, K_1 .

Thus, Figs 11 and 14 represent about the best that the present calculations can achieve and the remaining differences must be ascribed to uncertainties in the experimental data and incomplete representation of the problem in the calculations. The first of these is discussed in Ref 1 and stems from the problems of extracting small differences from tests carried out over extended time-scales using balances of varying accuracy. Likely sources of error in the calculations are the absence of the fuselage, poor representation of the span loading (no flap cut-outs), the lack of any allowance for the (wing) lift constraint sidewash at the strut guard and the absence of any modelling of the displacement effect of the strut guard wakes.

7 CONCLUSIONS

This investigation of the lift interference effects of under-wing strut guards has clarified the mechanisms involved and has been much more successful than the earlier attempt[1] made using vortex lattice calculations. In particular, the rather unexpected reduction in interference with increase in lift beyond a certain value has been accounted for by a sweep dependent, nonlinear lift contribution. The level of agreement between theory and experiment has shown that both the mutual lift and the displacement effects need to be considered. Further comparisons between the calculation method and experiment are necessary to establish how much of the remaining discrepancy in the present calculations is due to the shortcomings of the method and how much to uncertainties in the experimental data. Comparison for a significantly different sweep angle and higher lift would be particularly useful. Nevertheless, the present results are encouraging and hold

out the prospect of predicting at least some aspects of the model support system lift interference on wings through the use of fairly simple panel method calculations.

LIST OF SYMBOLS

C_L	lift coefficient
C_ℓ	sectional lift coefficient
C_{YG}	guard side force coefficient
ΔC_L	overall lift interference
ΔC_ℓ	sectional lift interference
K	constant
K_1, K_2, K_3	constants
q	resultant velocity
x,y,z	cartesian axes with origin at the wing apex
α	incidence
$\overline{\Delta\alpha}$	effective mean interference incidence
γ	vortex strength
ρ	density

REFERENCES

No.	Author	Title, etc
1	D.A. Kirby A.G. Hepworth P.J. Butterworth	Some aspects of the aerodynamic interference of model support systems in the 5 metre Wind Tunnel. Unpublished MOD(PE) report
2	B. Maskew	The calculation of potential flow aerodynamic characteristics of combined lifting surfaces with relaxed wakes. BAe Kingston-Brough, Note No.YAD 3192, September 1973
3	J.A.H. Petrie	A surface source and vorticity panel method. Aero Quarterly, Vol XXIX, November 1978
4	M. Saiz C. Quemard	Airbus A310: Essais dans la soufflerie F1 de l'ONERA: Comparaison vol-soufflerie, Paper 22 in AGARD CP-348 (1984)
5	H.C. Garner E.W.E. Rogers W.E.A. Acum E.C. Maskell	Subsonic wind tunnel wall corrections. AGARDograph 109, October 1966

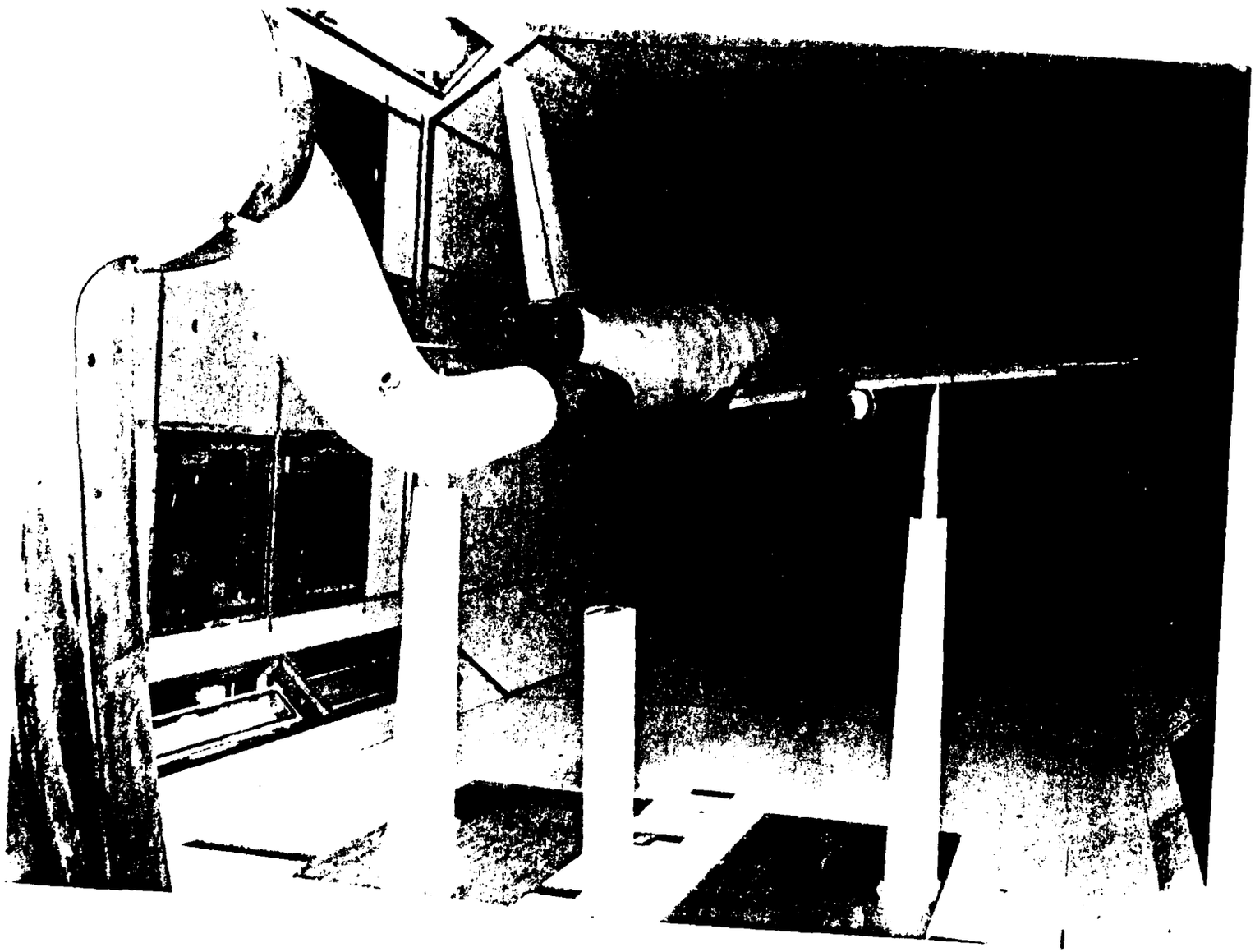

Fig 1 A300B model mounted on the sting cart with guards and dummy struts in position

Fig 2

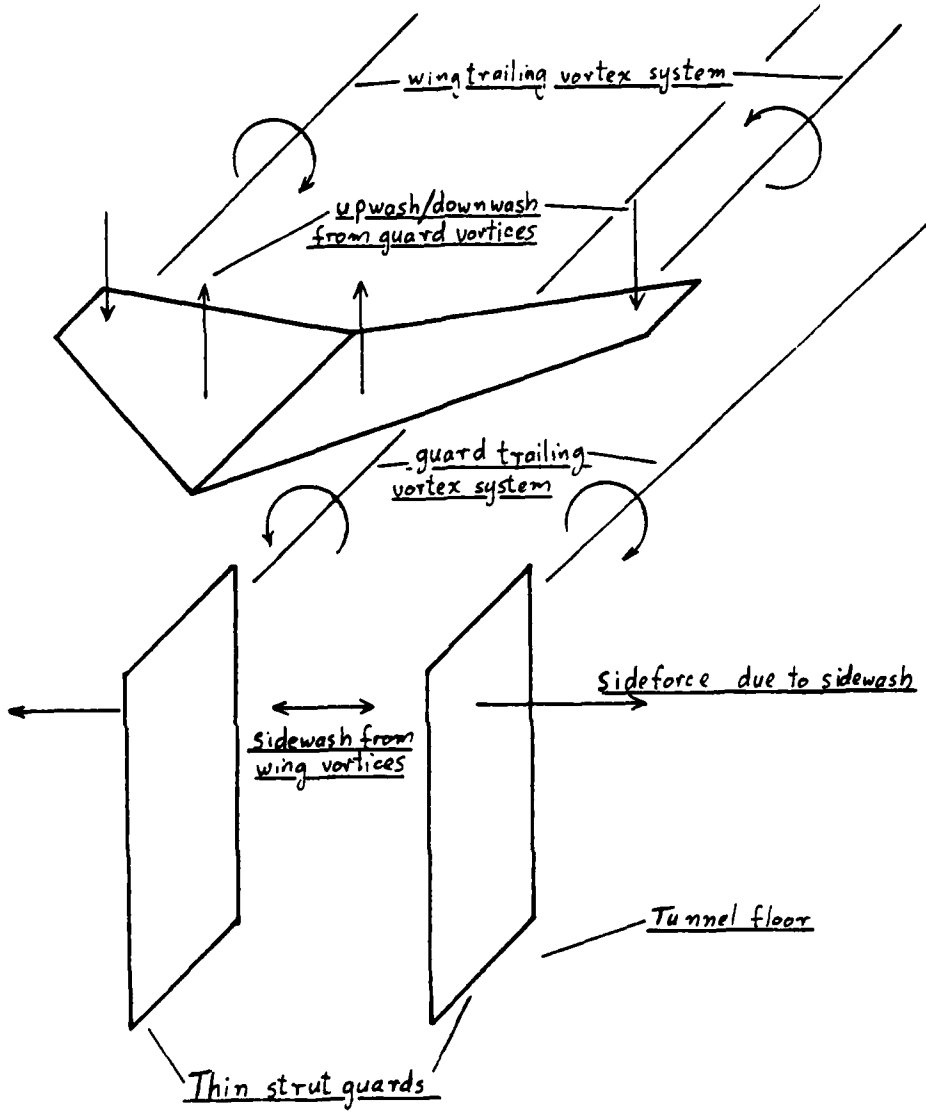

Fig 2 Mutual lift interference between wing and strut guards

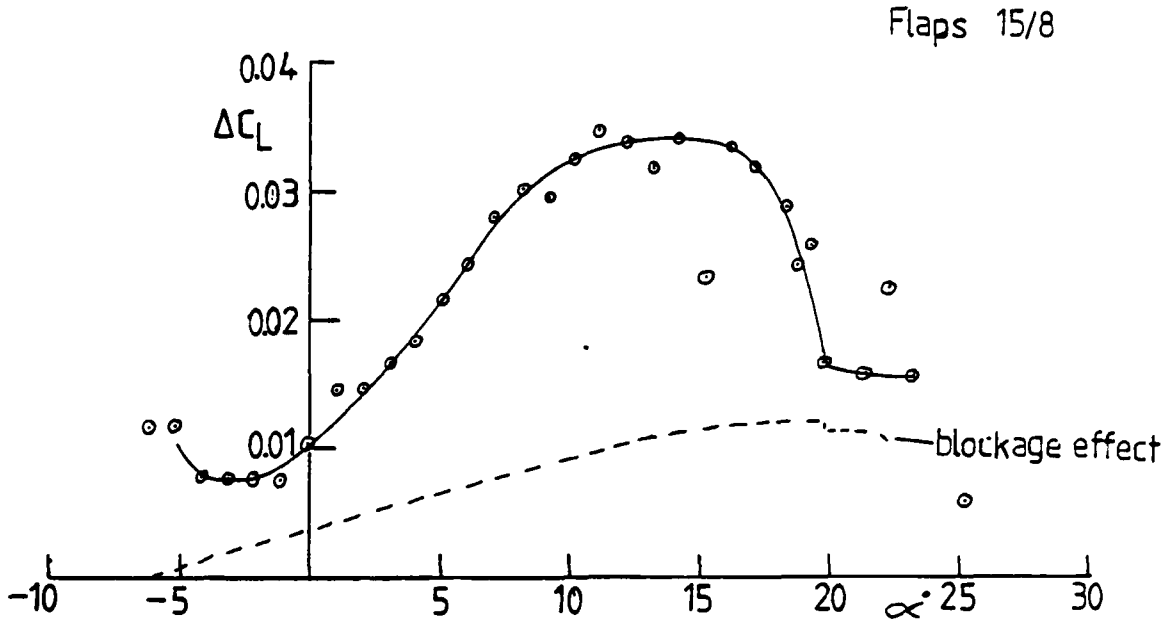

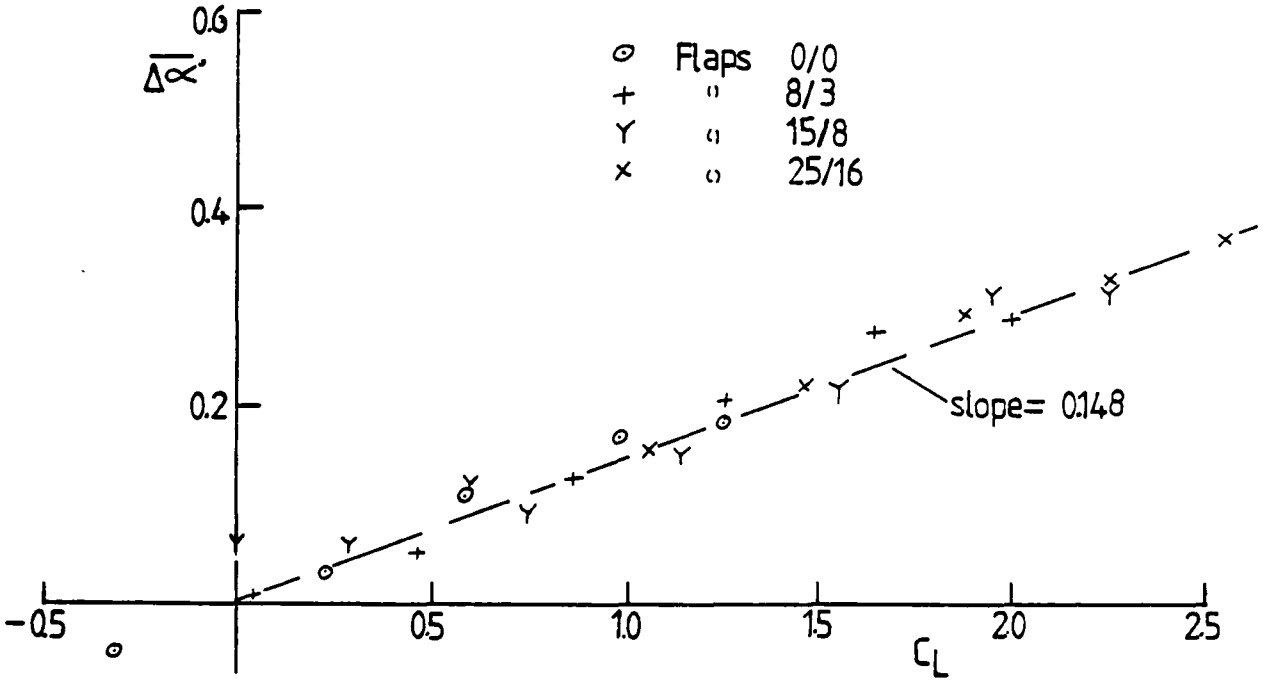

Fig 3 Results (Figs 11 and 15) from Ref 1

Fig 4

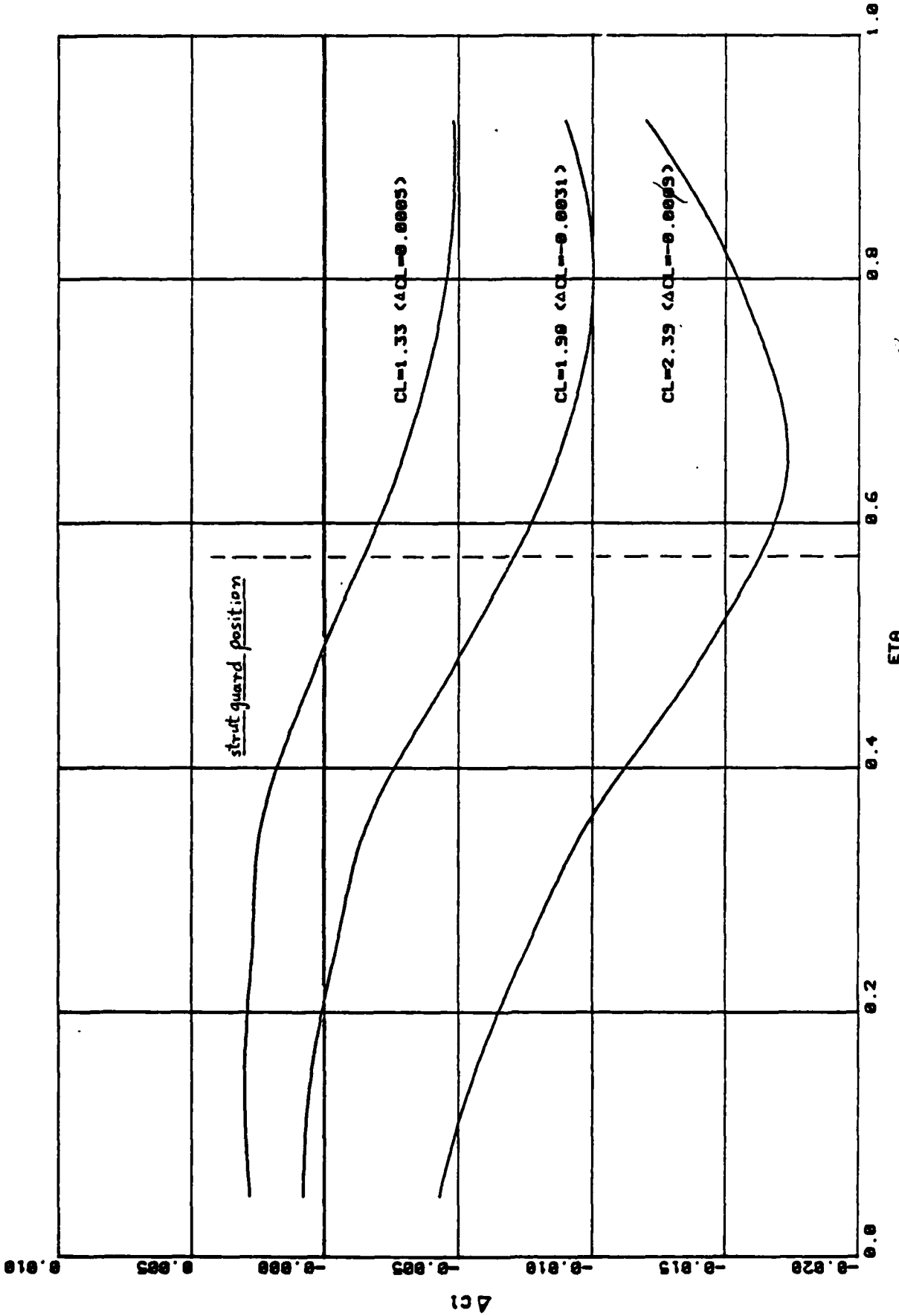

Fig 4 SPARV calculation for thin guard lift interference on simplified A300B geometry

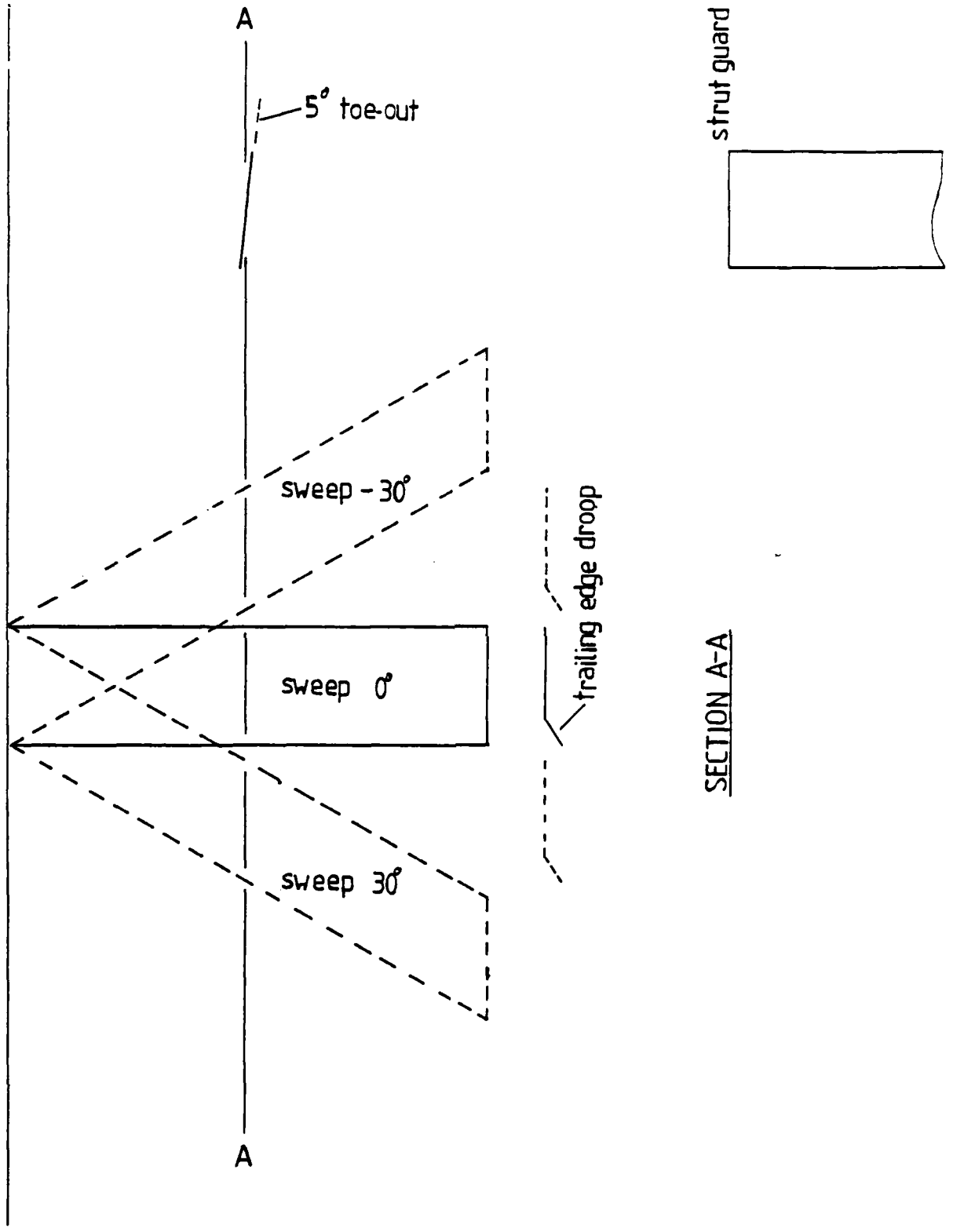

Fig 5 Geometry used for fixed sideforce strut guard calculations

Fig 6a&b

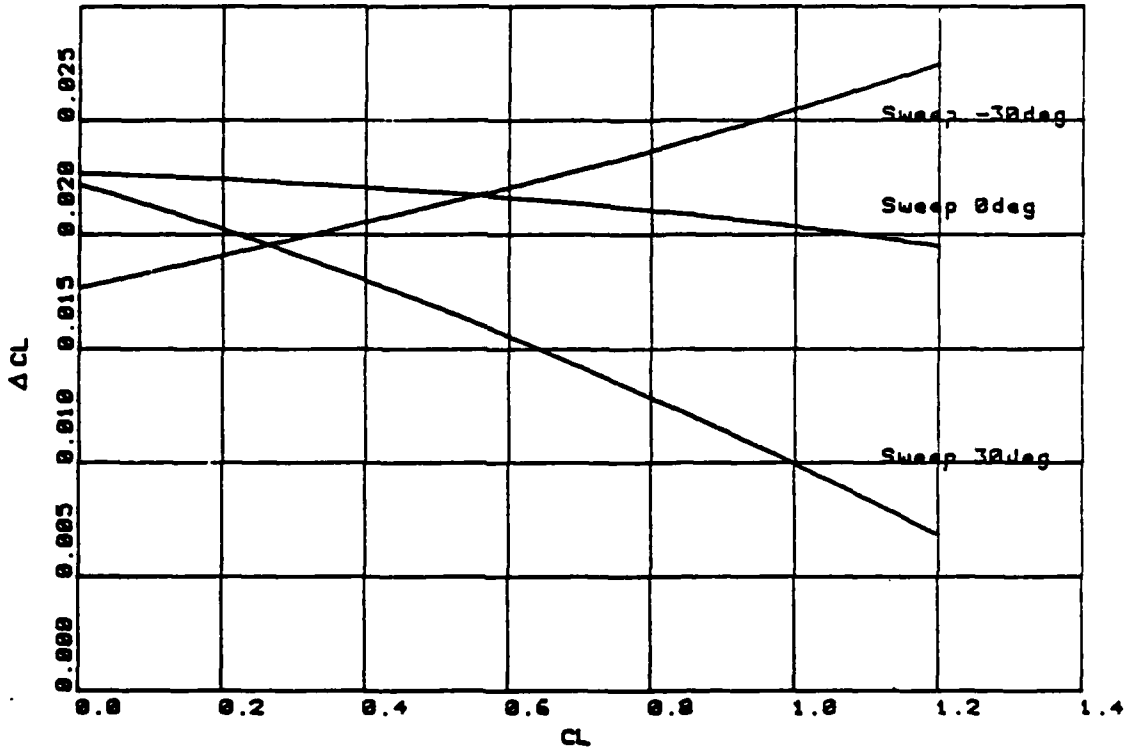

Fig 6a Effect of wing sweep on interference due to a thin guard with fixed side force

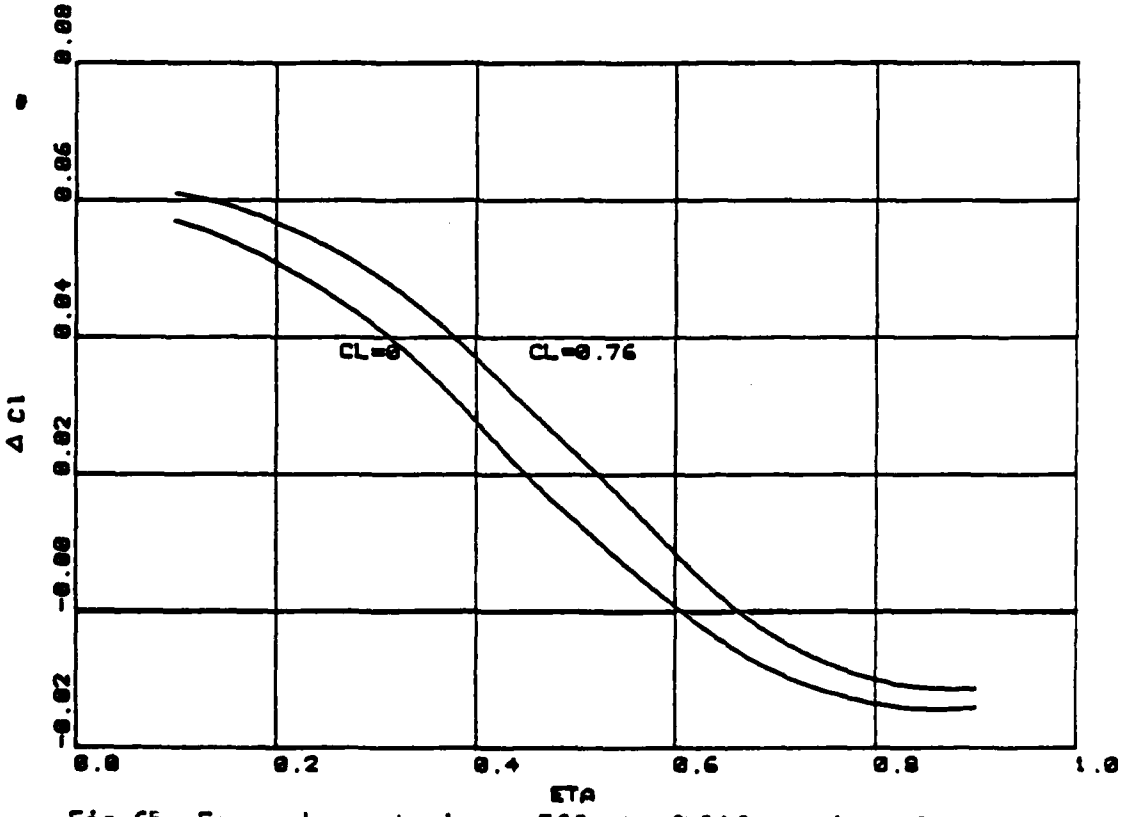

Fig 6b Forward swept wing. Effect of lift on interference effect ~~on~~ of thin guard.

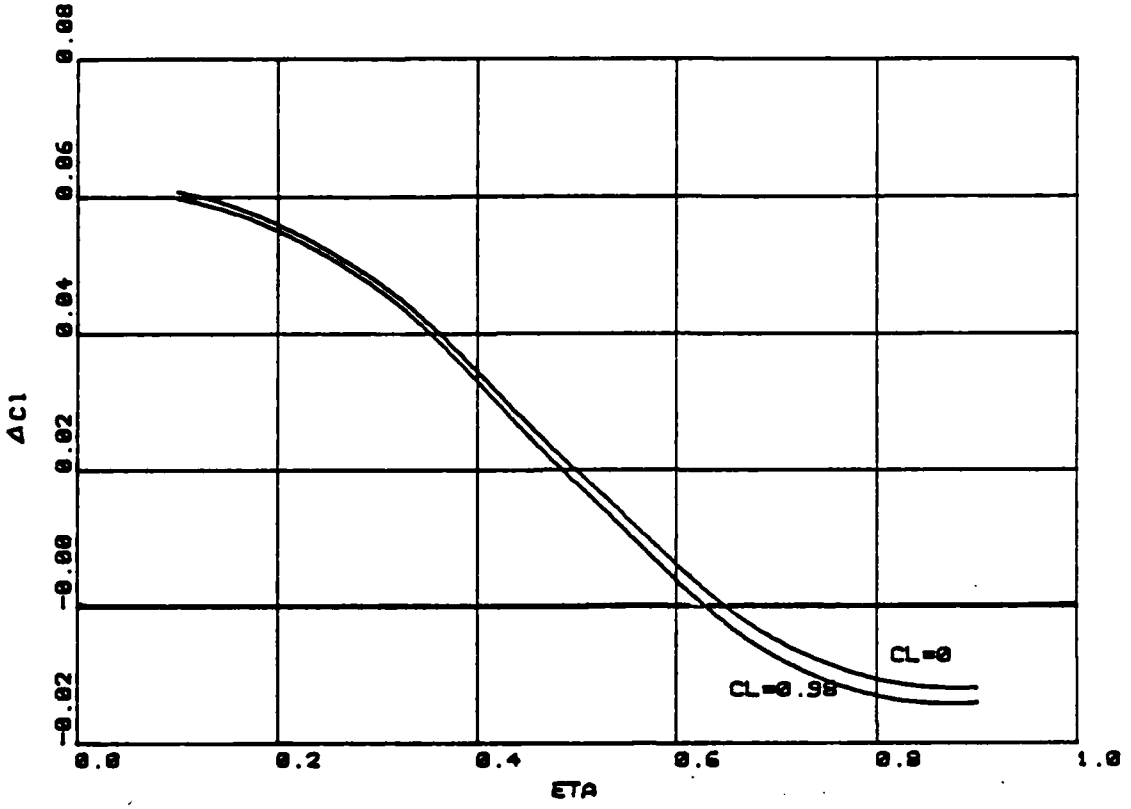

Fig 6c Unswept wing. Effect of lift on interference effect of thin guard

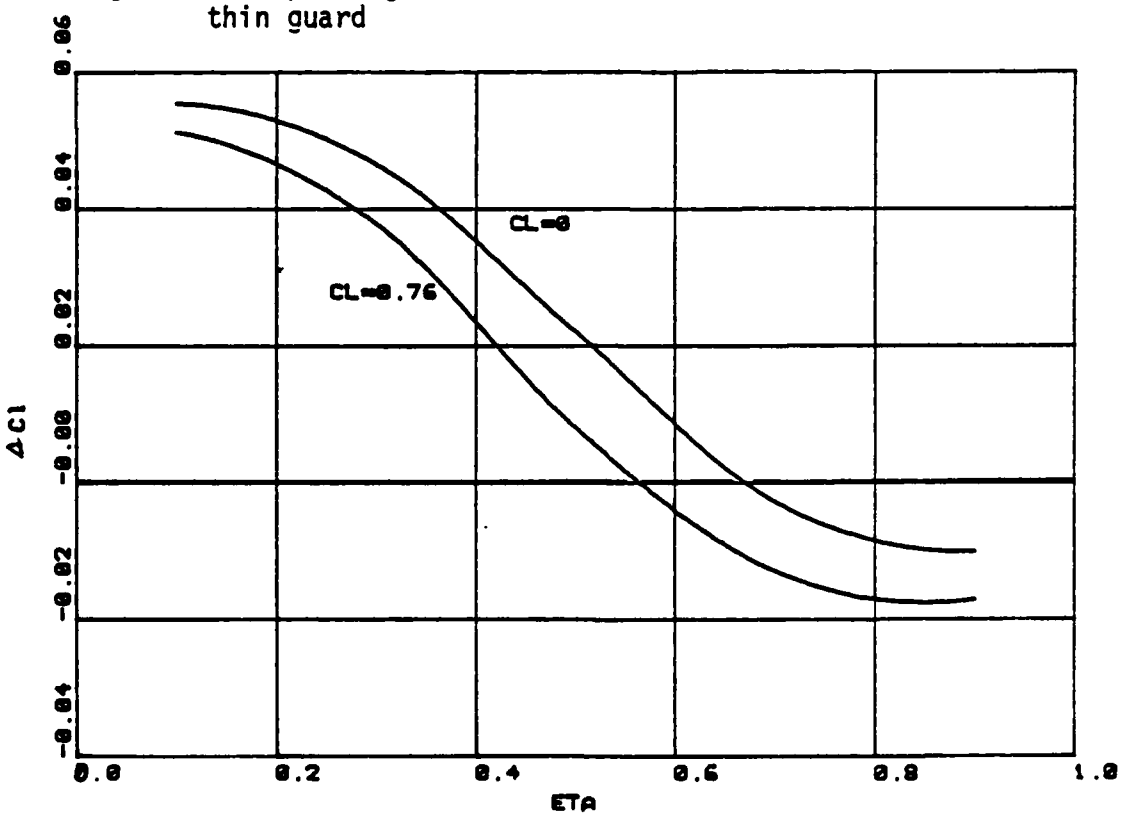

Fig 6d Aft swept wing. Effect of lift on interference effect of thin guard

Fig 7

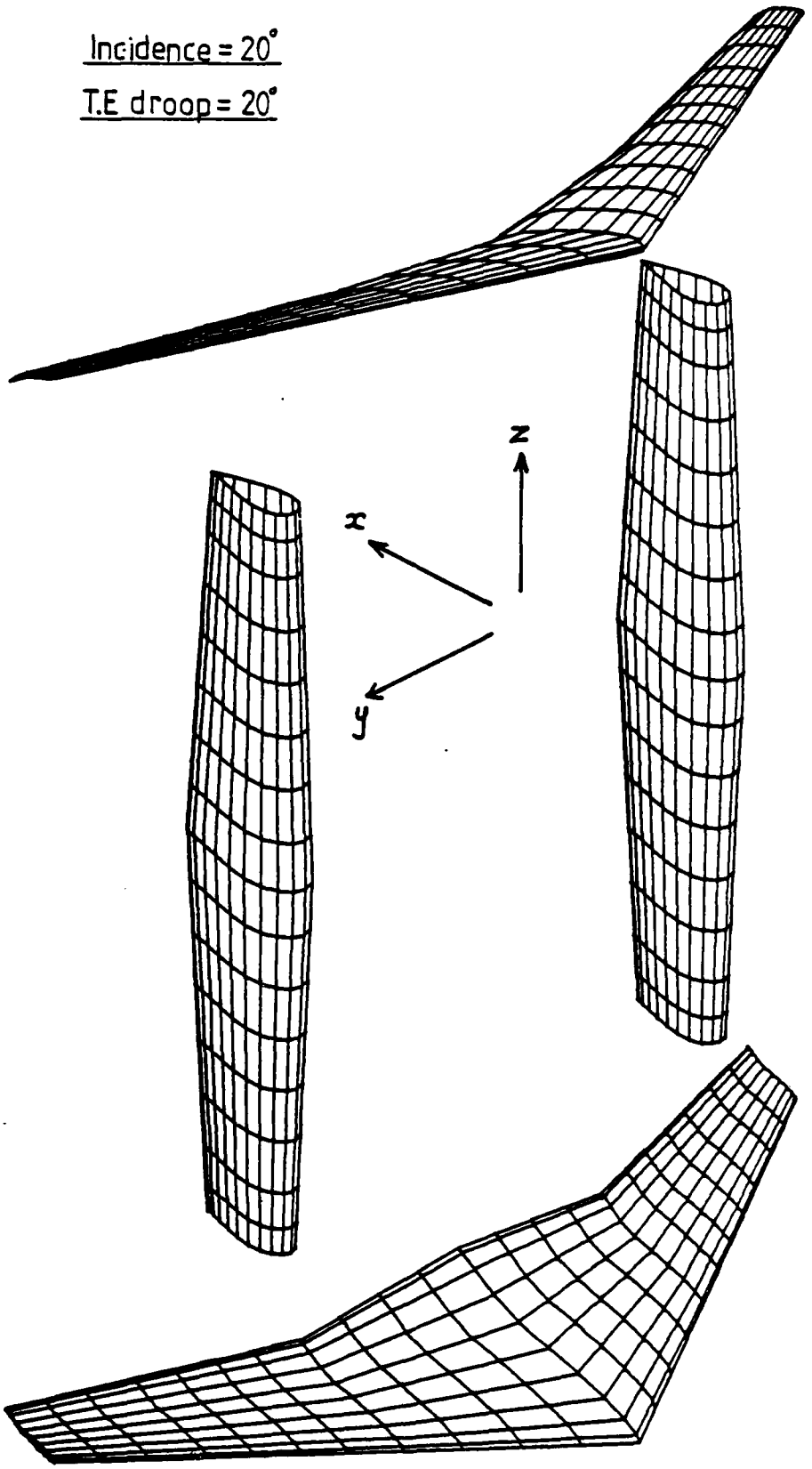

Fig 7 A300B panelling for SPARV calculations

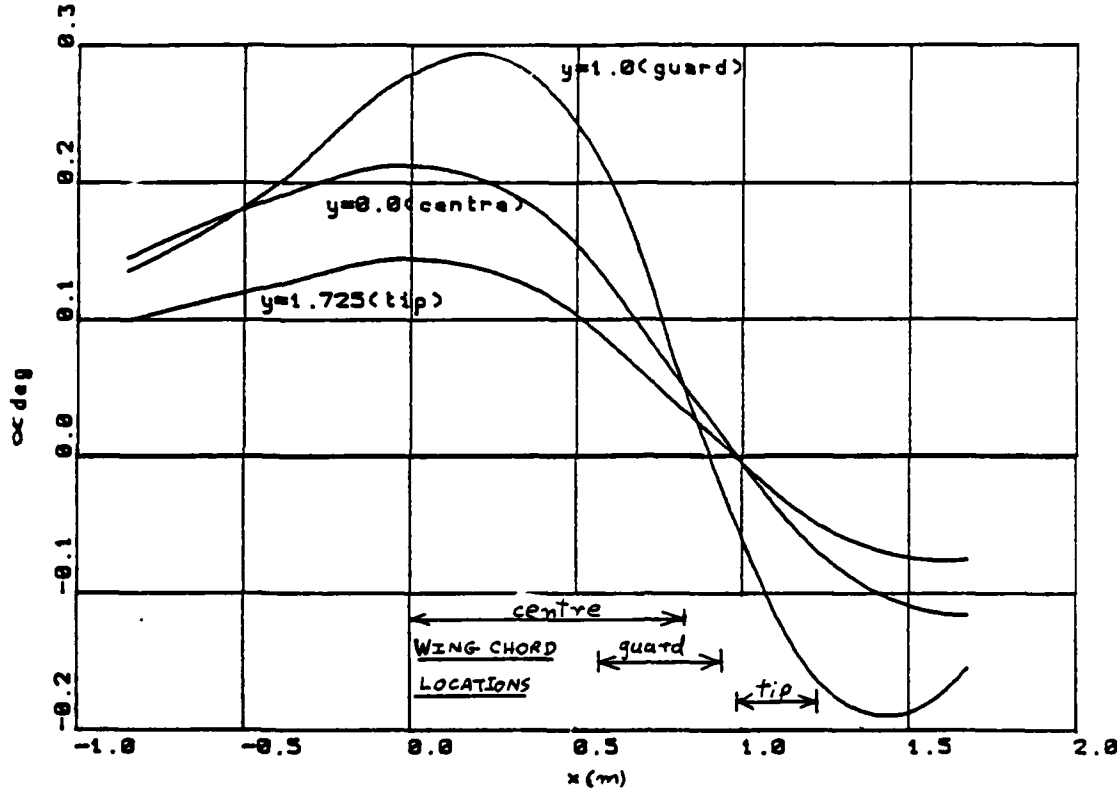

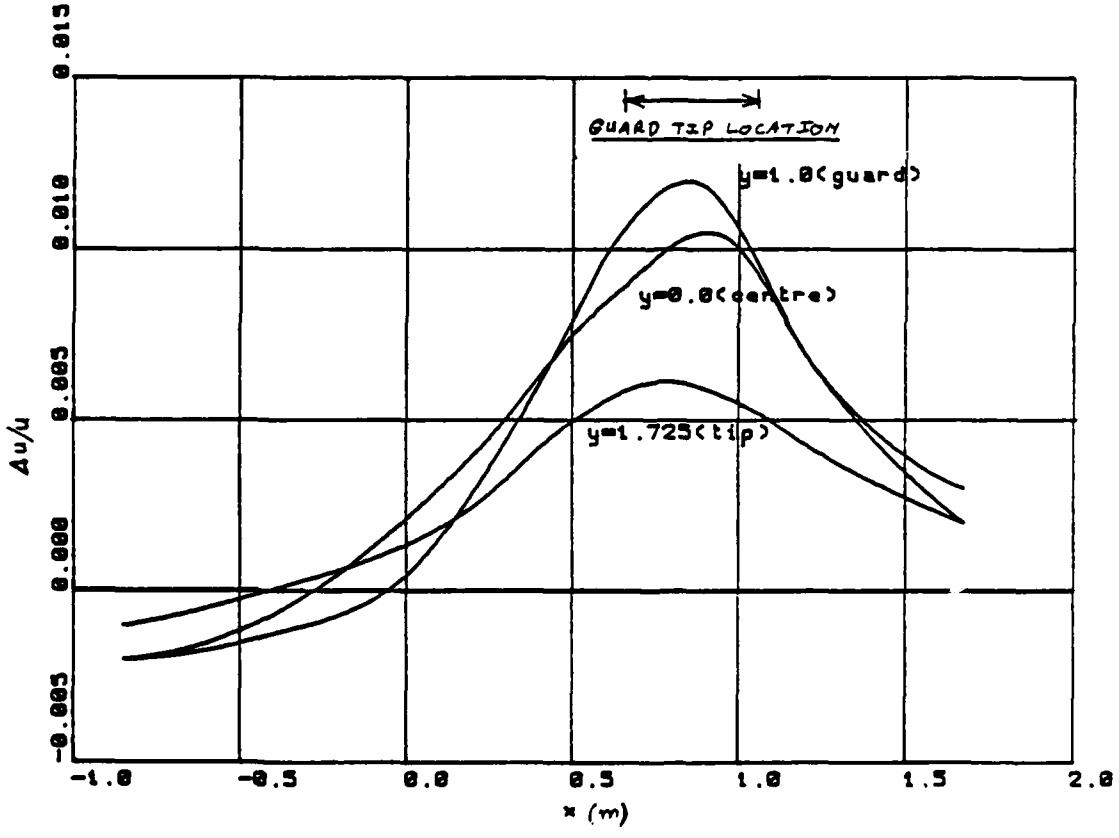

Fig 8 A300B interference velocities in the wing plane due to guard displacement effects

Fig 9

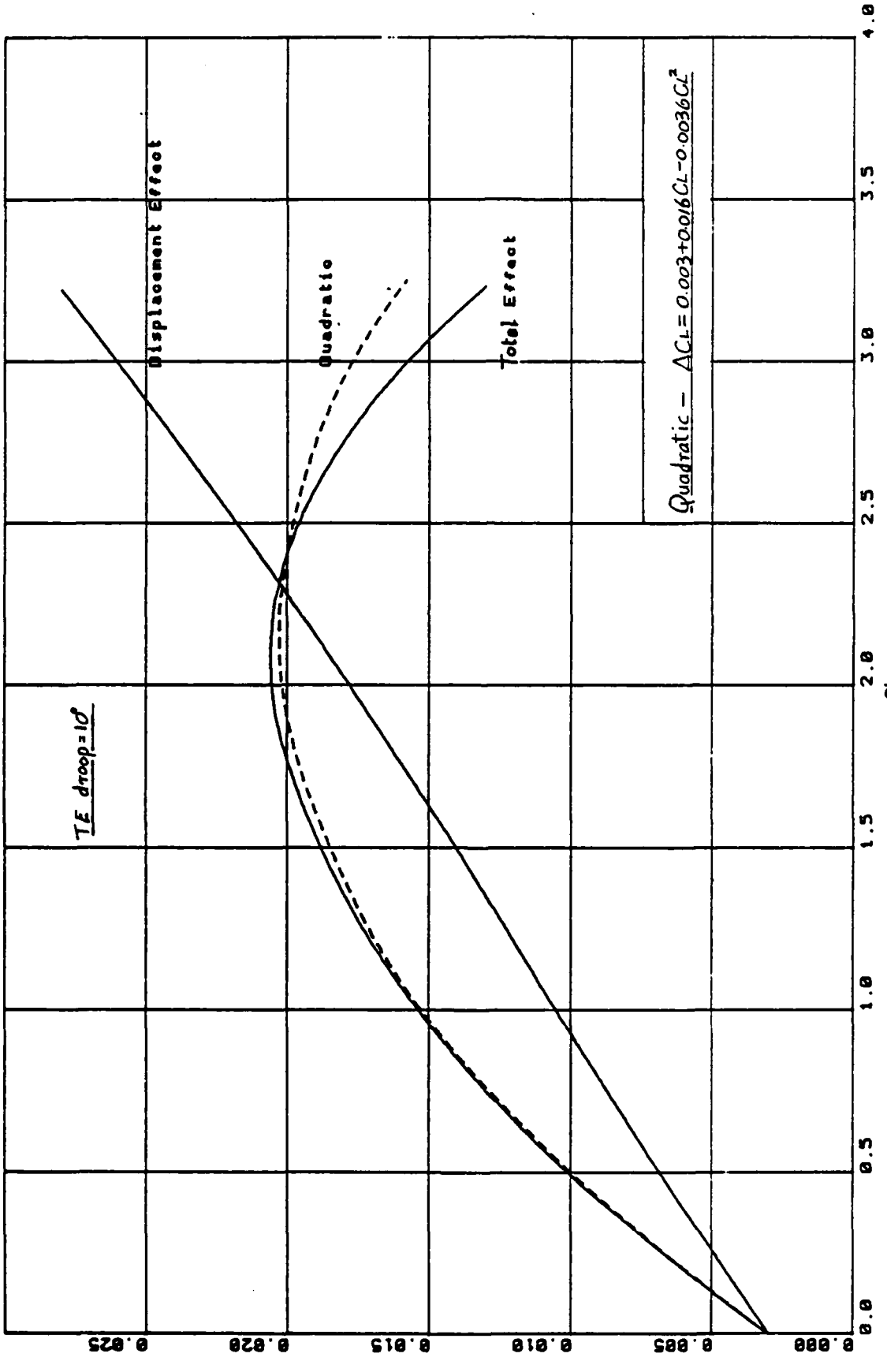

Fig 9 SPARV calculation of overall and displacement (thick guard - thin guard) effects for A300B

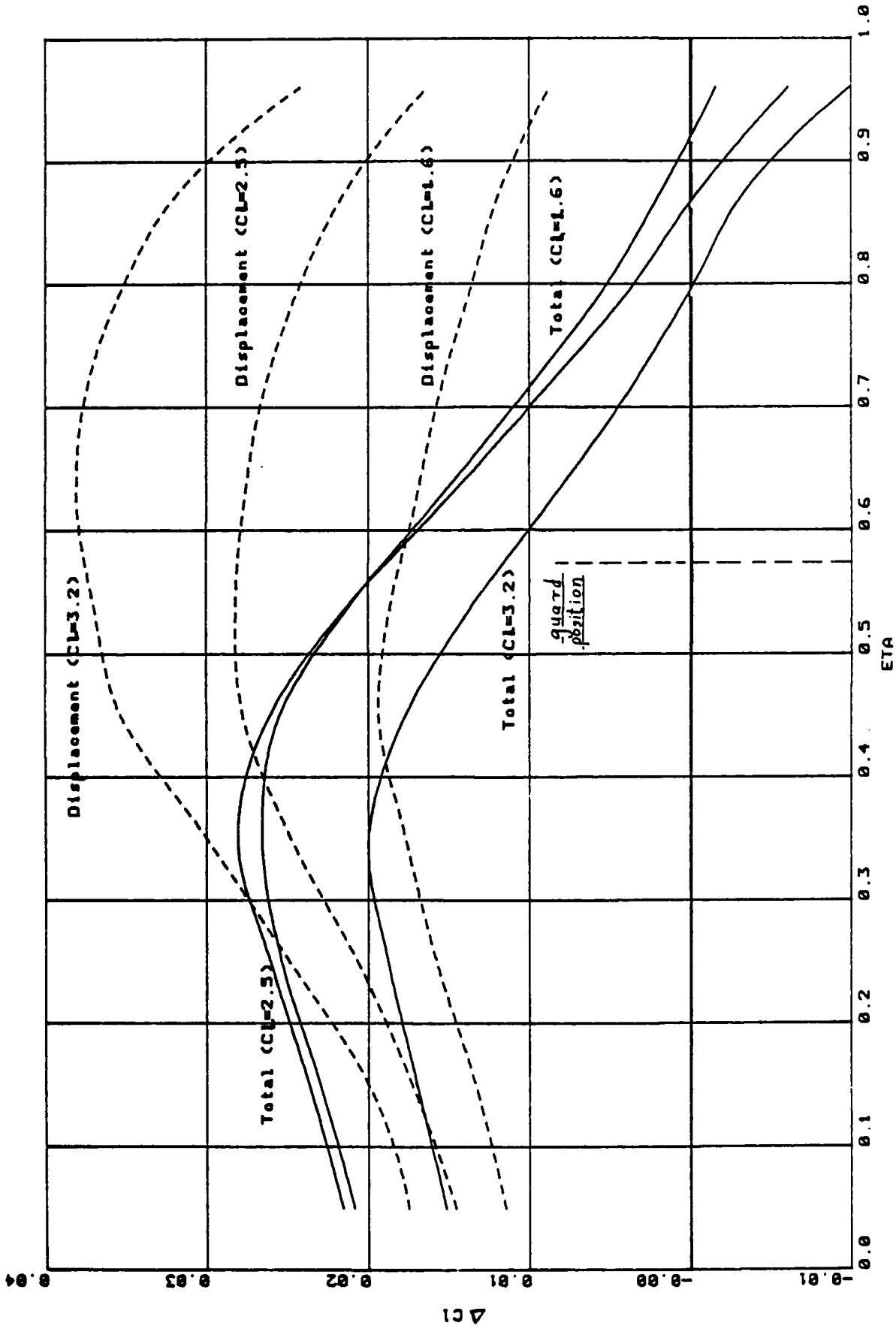

Fig 10 SPARV calculation of spanwise variation of overall and displacement (thick guard - thin guard) effects for A300B

Fig 11

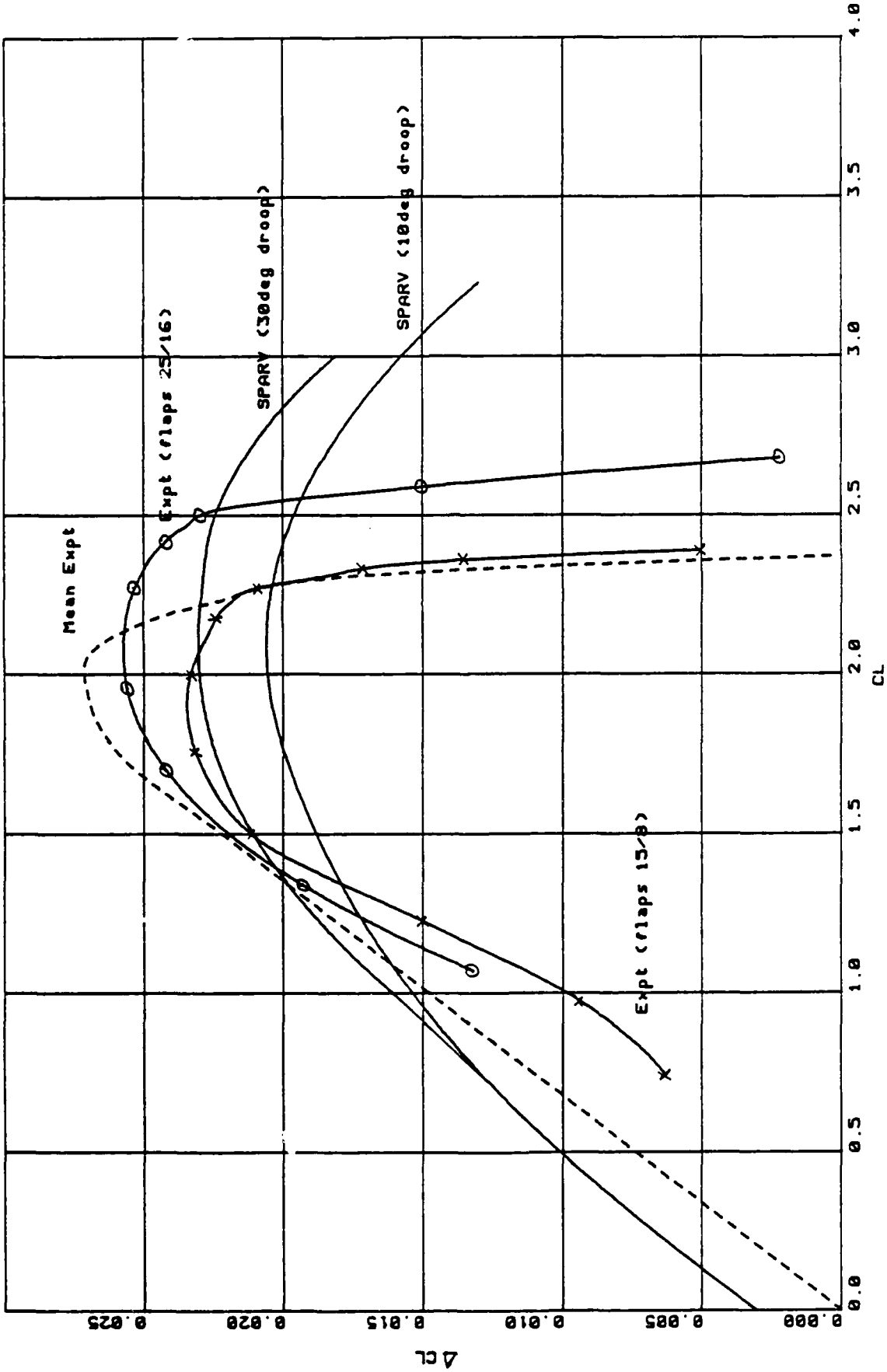

Fig 11 Comparison of SPARV calculation with experiment of Ref 1 for A300B

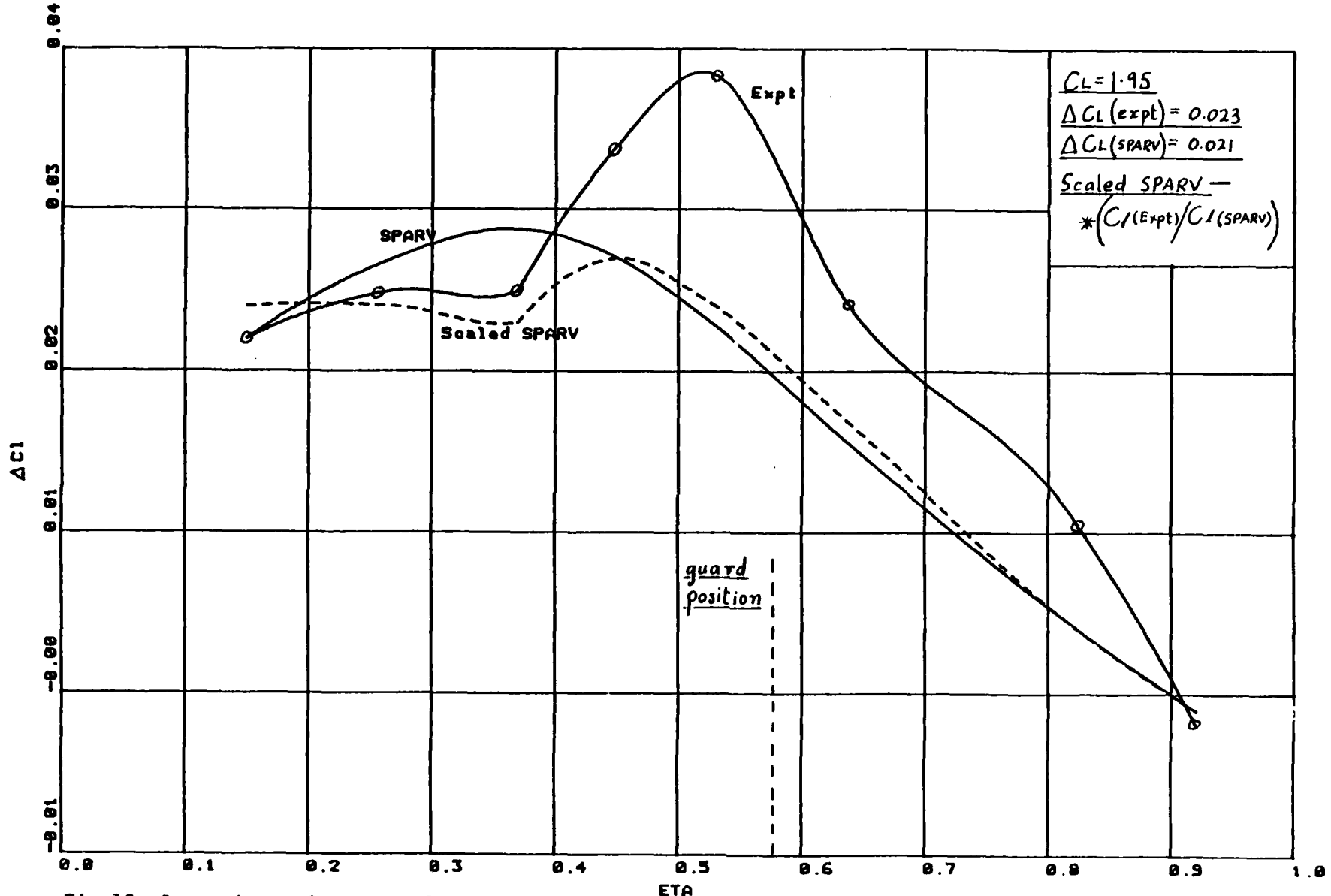

Fig 12 Comparison of SPARV calculation with experiment of Ref 1 for A300B

Fig 12

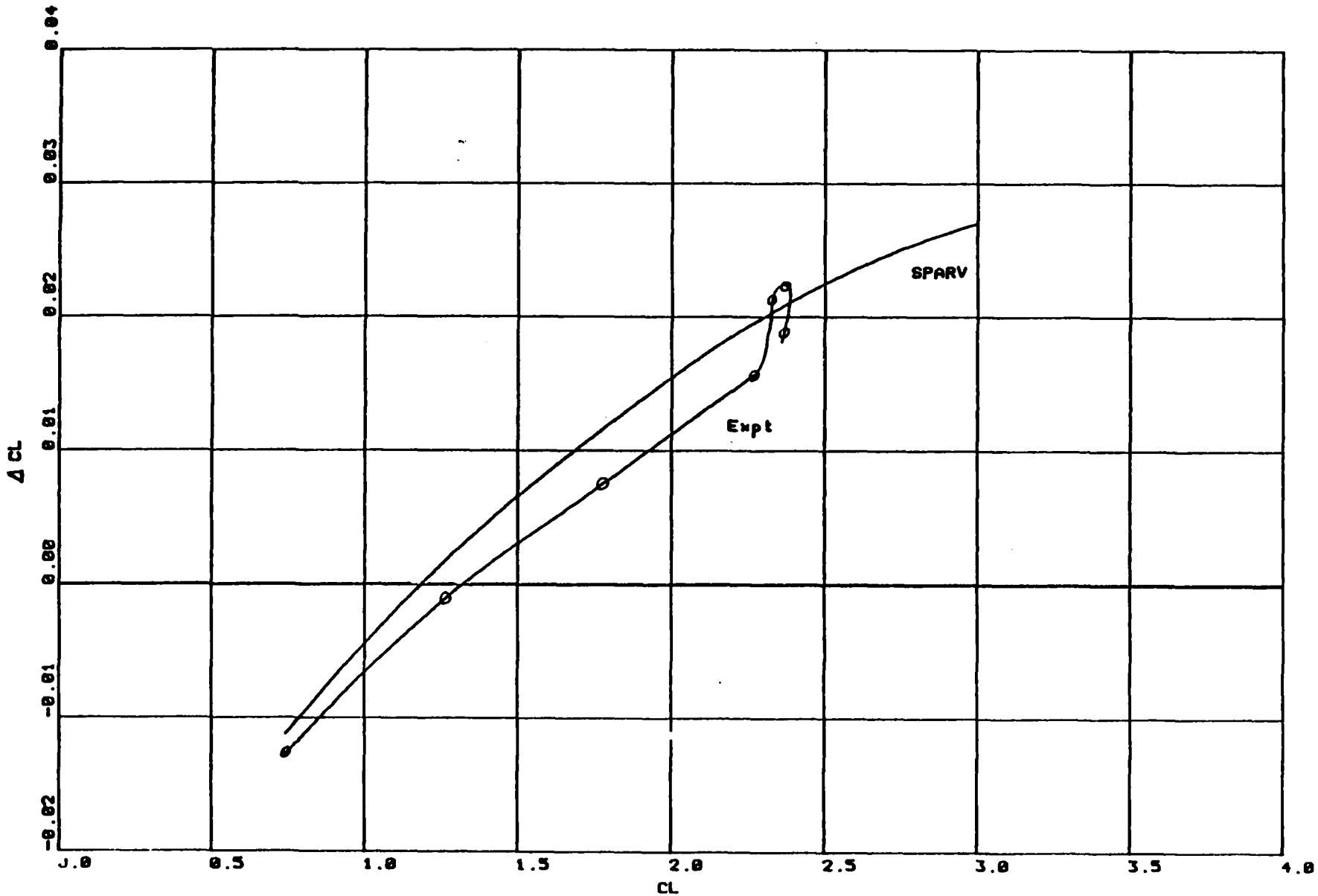

Fig 13 Comparison of SPARV calculation with experiment of Ref 1 for A300B with guards set at 5 deg

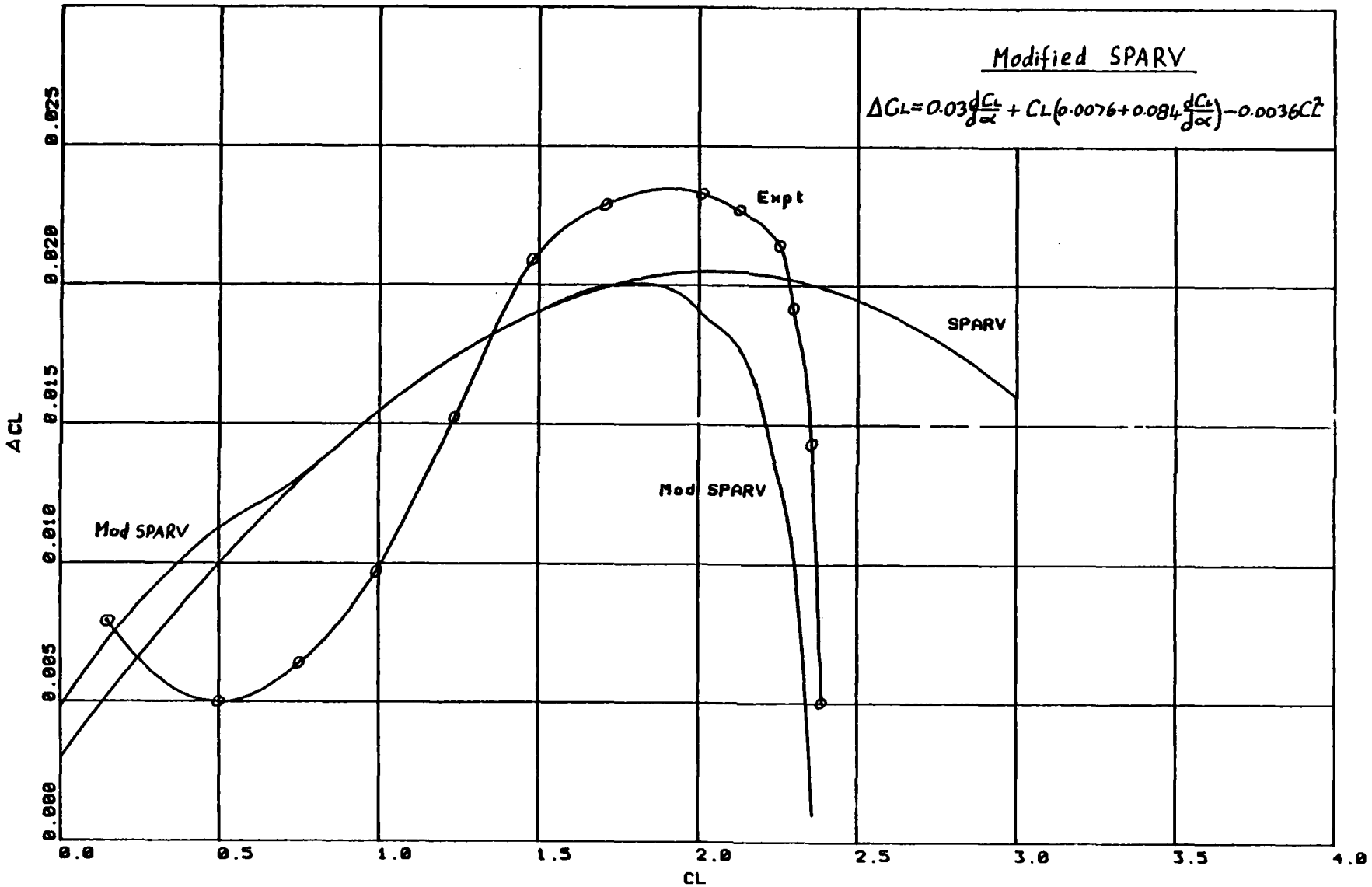

Fig 14 Comparison of modified SPARV results with experiment of Ref 1 for A300B

REPORT DOCUMENTATION PAGE

Overall security classification of this page

UNCLASSIFIED UNLIMITED

As far as possible this page should contain only unclassified information. If it is necessary to enter classified information, the box above must be marked to indicate the classification, e.g. Restricted, Confidential or Secret.

1. DRIC Reference (to be added by DRIC)	2. Originator's Reference	3. Agency Reference	4. Report Security Classification/Marking
	RAE TM Aero 2046	N/A	UNLIMITED

5. DRIC Code for Originator	6. Originator (Corporate Author) Name and Location
7673000W	Royal Aircraft Establishment, Farnborough, Hants, UK
5a. Sponsoring Agency's Code	6a. Sponsoring Agency (Contract Authority) Name and Location
N/A	N/A

7. Title A numerical study of the aerodynamic interference of a model support system used in the RAE 5 metre Tunnel

7a. (For Translations) Title in Foreign Language

7b. (For Conference Papers) Title, Place and Date of Conference

8. Author 1. Surname, Initials	9a. Author 2	9b. Authors 3, 4	10. Date	Pages	Refs.
Hardy, B.C.			September 1985	28	5

11. Contract Number	12. Period	13. Project	14. Other Reference Nos.
N/A	N/A		

15. Distribution statement

(a) Controlled by – Head of Aerodynamics Department, RAE

(b) Special limitations (if any) –

16. Descriptors (Keywords) (Descriptors marked * are selected from TEST)

Wind tunnels*. Subsonic flow*. Aerodynamic characteristics*.

17. Abstract

Some aspects of the lift interference effects of support systems for wind-tunnel models have been investigated using panel method calculations. The mechanisms involved have been clarified and comparison with experimental results for a large civil transport model in the RAE 5 metre Tunnel is encouraging.

F5910/1

DTIC

END

4-86